Energy band and spin-dependent many-body interactions in ferromagnetic Ni(110): A high-resolution angle-resolved photoemission study

Mitsuharu Higashiguchi,[1] Kenya Shimada,[2,*] Keisuke Nishiura,[3] Xiaoyu Cui,[1] Hirofumi Namatame,[2] and Masaki Taniguchi[1,2]
[1]*Graduate School of Science, Hiroshima University, Higashi-Hiroshima 739-8526, Japan*
[2]*Hiroshima Synchrotron Radiation Center, Hiroshima University, Higashi-Hiroshima 739-0046, Japan*
[3]*Faculty of Science, Hiroshima University, Higashi-Hiroshima 739-8526, Japan*
(Received 16 August 2005; published 30 December 2005)

High-resolution angle-resolved photoelectron spectroscopy of ferromagnetic Ni(110) has been conducted to elucidate energy band and spin-dependent many-body interactions. A kink structure has been clearly observed in the energy band dispersions of the minority spin $\Sigma_{2\downarrow}$ and $\Sigma_{1\downarrow}$, while it is absent in the majority spin $\Sigma_{1\uparrow}$ band. Analyses of the self-energy indicate that the kink originates from the electron-phonon interaction. Based on a detailed study of the effective mass enhancement, we find that the electron-phonon interaction and electron correlation contribute to the spectral features near the Fermi level in different ways, depending on the identity of the energy band and the spin direction. These results provide insight into the interplay of these many-body interactions on quasiparticles near the Fermi level.

DOI: 10.1103/PhysRevB.72.214438 PACS number(s): 75.25.+z, 75.10.Lp, 79.60.Bm, 71.18.+y

In the past decade, the energy and angular resolutions of photoelectron spectroscopy have been vastly improved.[1–3] Now we can examine electronic fine structures near the Fermi level (E_F), which are directly related to low energy excitations in the solid. For the investigation of many-body interactions in quasiparticles, high-resolution angle-resolved photoelectron spectroscopy (ARPES) is a sophisticated tool. In this spectroscopy, the major spectral features are given by the single-particle spectral function $A^\sigma(k,\omega)$, which is related to the imaginary part of the single-particle Green's function $A^\sigma(k,\omega)=-(1/\pi)\mathrm{Im}\,G^\sigma(k,\omega)=-(1/\pi)\mathrm{Im}\{1/[\omega-\epsilon_k^0-\Sigma^\sigma(k,\omega)]\}$, where σ and ϵ_k^0, respectively, represent the spin and the energy of the noninteracting band.[1–3] The imaginary part ($\mathrm{Im}\,\Sigma^\sigma$) and real part ($\mathrm{Re}\,\Sigma^\sigma$) of the self-energy can be evaluated, respectively, from the spectral width (δE) and the energy shift from ϵ_k^0.[1–3] By means of the ARPES spectra, therefore, the self-energy $\Sigma^\sigma(k,\omega)$, in which all the many-body interactions are involved, can be evaluated directly.

Recently, a "kink structure" (or a sudden change of the Fermi velocity, $v_F=1/\hbar(dE/dk)_{k=k_F}$) in high-$T_c$ cuprates has attracted much interest, since it is regarded as an important clue to an understanding of the many-body interactions responsible for high-T_c superconductivity.[2] Although it is widely believed that the kink structure is related to a bosonic mode such as a phonon or magnetic excitation,[2] the nature of this mode has not yet been clarified. One of the reasons for this difficulty is that the characteristic energy scales for these excitations are similar and only one Fermi surface is available for detailed analyses. An examination of a magnetic and multiband system may produce insights into the respective contributions from these excitations.

On the other hand, many studies exist on the kink structure derived from the electron-phonon interaction in the surface electronic states of metals.[3,4] However, in order to relate the fine spectral features with the bulk physical properties obtained from magnetic and transport measurements, one should examine energy bands derived from the bulk electronic states. In addition, electron correlation is not significant for these surface states.

We, therefore, selected ferromagnetic Ni as a suitable subject of study, since it has spin-polarized Fermi surfaces where quasiparticles with different effective masses exist. Furthermore, the importance of electron correlation in the spin-polarized Ni 3*d* bands has been well established from unusual spectral features, such as the 3*d* reduced band widths and exchange splittings reported by ~25% (Refs. 5–9) and ~50% (Refs. 5–9) compared with those given by band-structure calculations with the local spin-density approximation (LSDA),[10,11] and the existence of a spin-polarized 6 eV satellite.[12–15]

We should also note that the electronic band structure of Ni is conveniently simple from a theoretical point of view; most of the majority-spin 3*d* states of Ni are occupied, and less than one hole exists in the minority-spin 3*d* states. Kanamori considered electron correlation effects on the ferromagnetism of Ni taking into account the multiple scattering of two particles.[16] Penn calculated the value of $A^\sigma(k,\omega)$ based on this picture, and interpreted the 6-eV satellite as the "two-hole-bound state."[17] The narrowing and the reduced exchange splittings of the Ni 3*d* bands are explained in terms of the electron correlation effect.[18–20] However, experimental examinations of the self-energy, needed to verify these theoretical considerations, have not as yet been performed.

In this paper, we present a high-resolution low-temperature ARPES study on Ni, and evaluate the self-energy of the valence bands ($\Sigma_{2\downarrow}$, $\Sigma_{1\uparrow}$, and $\Sigma_{1\downarrow}$) forming the Fermi surface along the high-symmetry line ΓKX. A kink structure is clearly observed only for the minority-spin bands. On the basis of the quantitative analyses of the self-energy, we examine the origin of the kink structure in detail. Having also appraised the respective contributions of the electron-phonon and electron correlation to an effective electron mass (m^*) enhancement, we elucidate the significant energy band and spin-dependence of these interactions.

The experiments were performed on the undulator beamline (BL-1) of a compact electron-storage ring (HiSOR) at Hiroshima University.[21] The high-resolution ARPES mea-

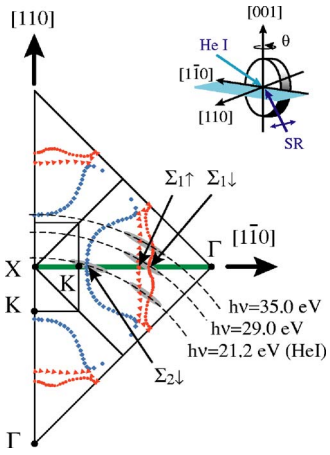

FIG. 1. (Color online) A schematic view of the geometry of the present experiment, and the Brillouin zone of Ni in the extended zone scheme. The $\Sigma_{2\downarrow}$, $\Sigma_{1\uparrow}$, and $\Sigma_{1\downarrow}$ bands crossing the ΓKX line (along the green line) were examined. Small symbols indicate the Fermi surface obtained from a de Haas–van Alphen measurement (after Ref. 10).

surements were carried out using an angular mode of a hemispherical electron-energy analyzer (ESCA200, SCIENTA). A depolarized He resonance line ($h\nu$=21.2 eV: He I) and a linearly polarized undulator radiation ($h\nu$=29.0 and 35.0 eV) were used as excitation photons. The total energy resolution was set at ΔE=6 meV ($h\nu$=21.2 eV), and 11 meV ($h\nu$=29.0 and 35.0 eV), and the angular resolution at $\Delta\theta=\pm 0.15°$ ($\Delta k_{\parallel}$=0.009–0.01 Å^{-1}). A single crystal of Ni(110) (99.999%) was cleaned by repeated cycles of Ar^+ ion sputtering (1 kV) and subsequent annealing at 500 °C. The amount of impurities such as C, O, and S on the surface was below the detection limit of Auger electron spectroscopy. Clear low-energy electron diffraction (LEED) spots confirmed that the atoms were well ordered and that no contaminants existed on the sample surface. The sample was mounted on a liquid-He–flow-type cryostat, and the sample temperature was set at 10 K. The base pressure of the main chamber was better than 5×10^{-11} Torr.

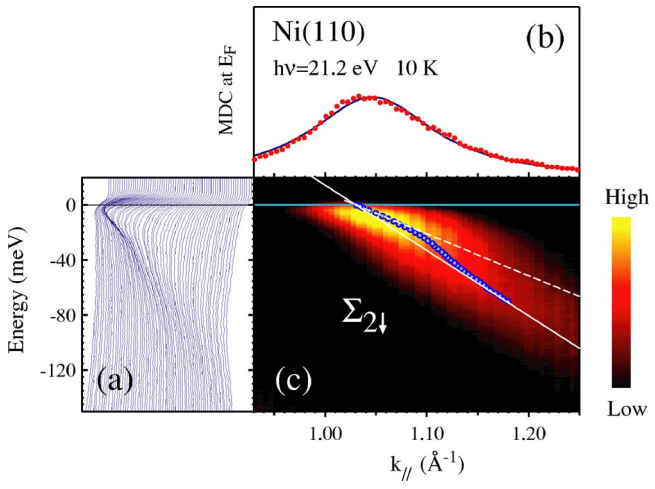

FIG. 2. (Color online) The ARPES results of Ni(110) at 10 K. (a) shows EDC's and (c) shows intensity plots for the $\Sigma_{2\downarrow}$ band. (b) shows MDC's near E_F obtained from EDC's. Circles and solid lines (white) in (c) indicate evaluated peak positions, and linear dispersions without the kink structure, respectively. Dashed lines show the gradient of the $\Sigma_{2\downarrow}$ band at E_F.

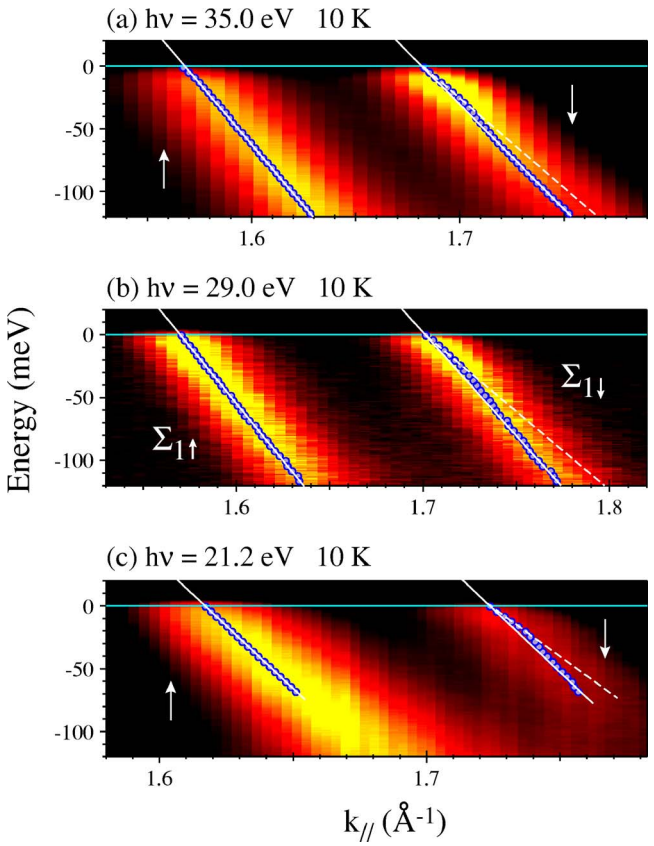

FIG. 3. (Color online) The ARPES intensity of Ni(110) at 10 K taken at $h\nu$=35.0 eV (a), 29.0 eV (b), and 21.2 eV (c). (b) shows the $\Sigma_{1\uparrow}$ and $\Sigma_{1\downarrow}$ bands. Circles and solid lines (white) indicate evaluated peak positions, and linear dispersions without the kink structure, respectively. Dashed lines in (a) and (b) show the gradient of the down-spin bands at E_F.

The ARPES measurements were performed by tuning the incident photon energy and by rotating the polar axis of the sample, parallel to the [001] direction for the (110) surface (Fig. 1).[22] In order to quantitatively examine the spectral shapes and compare the results with the LSDA calculation, we selected the ΓKX high symmetry line (Σ line), in which the majority-spin and minority-spin bands with the same or different symmetry could be examined simultaneously. The ARPES spectra of the $\Sigma_{2\downarrow}$ band were taken at $h\nu$=21.2 eV, and those of the $\Sigma_{1\uparrow}$ and $\Sigma_{1\downarrow}$ bands at $h\nu$=29.0 eV. The inner potential was assumed to be 10.7 eV.[8]

Figure 2(a) shows the energy distribution curves (EDC's), and Fig. 2(c) and Figs. 3(a)–3(c) provide the intensity plots. In order to quantitatively analyze the spectral shape, we used Lorentzians on a linear background [Fig. 2(b)] to fit the momentum distribution curves (MDC's)—the intensity distribution curves as a function of momentum for a given energy. The peak positions thus evaluated are indicated by circles in the intensity plots. One can recognize kink structures in the $\Sigma_{2\downarrow}$ [Fig. 2(c)] and $\Sigma_{1\downarrow}$ [Fig. 3(b)] bands, and in the minority-spin bands connected to the $\Sigma_{1\downarrow}$ band [Figs. 3(a) and 3(c)].

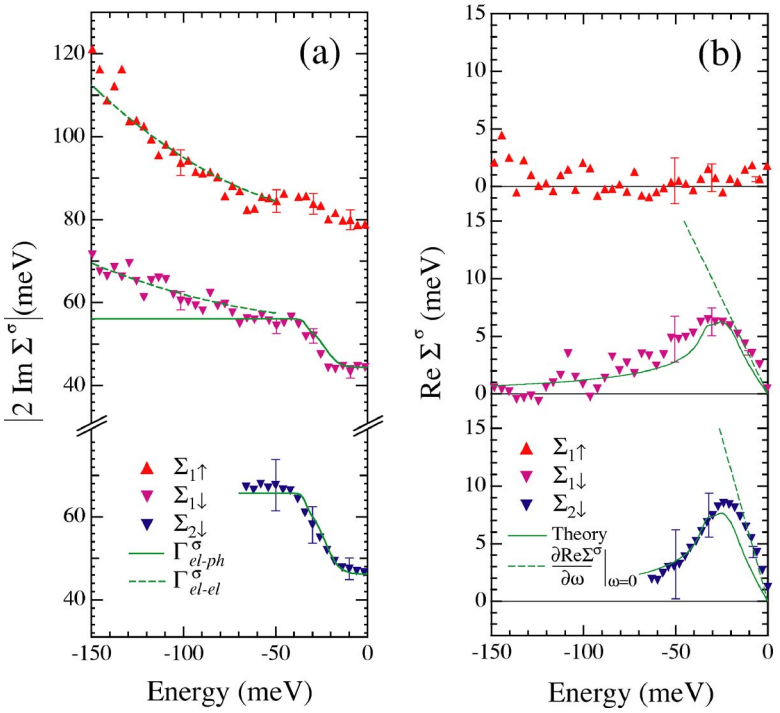

FIG. 4. (Color online) Experimentally obtained imaginary (a) and real (b) parts of the self-energy of the $\Sigma_{2\downarrow}$, $\Sigma_{1\uparrow}$, and $\Sigma_{1\downarrow}$ bands. Symbols represent the observed imaginary (real) parts of the self-energy. Solid and dashed lines in (a) exhibit theoretical $\Gamma_{el\text{-}ph}$ and $\Gamma_{el\text{-}el}$, respectively. Theoretical $\Gamma_{el\text{-}ph}+\Gamma_{el\text{-}el}$ in (a) are shifted by the offset Γ_0^σ. Solid and dashed lines in (b) indicate the theoretical Re $\Sigma^\downarrow$, and the gradients of experimental Re $\Sigma^\downarrow$ near E_F, respectively.

On the other hand, the kink structure is absent in the $\Sigma_{1\uparrow}$ band [Fig. 3(b)] and in the majority-spin bands connected to the $\Sigma_{1\uparrow}$ band [Figs. 3(a) and 3(c)].

In the present analyses, we used the MDC widths, δk's, to estimate the imaginary part, $|2\ \mathrm{Im}\ \Sigma^\sigma| = \delta E = (dE/dk)\delta k$.[23] We assumed that the band dispersion was linear when the kink structure was absent, as in the $\Sigma_{1\uparrow}$ band. In order to evaluate the linear band dispersions [solid lines in Figs. 2(c) and 3(b)], we estimated the gradient (dE/dk) by the fit of the experiments for the energy range less than −60 meV. To deduce the real part of the self-energy, we utilized the energy shifts from the linear band dispersions.

Figures 4(a) and 4(b) show the resulting self-energy components, Im Σ^σ and Re Σ^σ as symbols. The Im $\Sigma^\downarrow$ of the $\Sigma_{2\downarrow}$ and $\Sigma_{1\downarrow}$ bands are decreased for E > −40 meV, a finding which implies that the kink structures originate in the many-body interaction and not from the energy dispersion. Since the magnitude of the energy of the kink structures coincides well with the Debye temperature, $\Theta_D = 450$ K ($k_B\Theta_D = 39$ meV),[24] it is reasonable to assume that the structure is derived from the electron-phonon interaction.

In the case that the electron-scattering processes due to the electron-phonon, electron-electron, and electron-impurity interactions are independent, the lifetime broadening ($\Gamma^\sigma = |2\ \mathrm{Im}\ \Sigma^\sigma|$) of the quasiparticle can be expressed by the sum of each contribution: $\Gamma^\sigma = \Gamma^\sigma_{el\text{-}ph} + \Gamma^\sigma_{el\text{-}el} + \Gamma^\sigma_0$, where $\Gamma^\sigma_{el\text{-}ph}$ and $\Gamma^\sigma_{el\text{-}el}$ are the lifetime broadening due to the electron-phonon and electron-electron interactions, respectively,[1,3] and Γ^σ_0 represents an energy-independent term which should include the lifetime broadening derived from the electron-impurity scattering. In the case of photoemission from three-dimensional electron systems, the final-state lifetime broadening, which depends strongly on the incident photon energies, dominates spectral linewidth.[25–27] However, as shown below, since the observed energy dependence of the lifetime broadening can be explained well by $\Gamma^\sigma_{el\text{-}ph} + \Gamma^\sigma_{el\text{-}el}$ terms, we can reasonably assume that the energy dependence of the final-state lifetime broadening is negligible for the energy range $E = E_F \sim -150$ meV. We therefore regard the final-state lifetime broadening as a dominant part of Γ^σ_0 term, an energy-independent offset to Γ^σ.

Here, we concentrate our discussion on the energy-dependent peak widths derived from $\Gamma^\sigma_{el\text{-}ph} + \Gamma^\sigma_{el\text{-}el}$. The lifetime broadening due to the electron-phonon interaction is given by $\Gamma^\sigma_{el\text{-}ph} \cong 2\pi \int_0^\infty \alpha^2_{k\sigma} F(\nu)[2n(\nu,T) + f(\nu+\omega,T) + f(\nu-\omega,T)]d\nu$,[1,3] where $n(\nu,T)$ and $f(\nu,T)$ represent the Bose-Einstein and Fermi-Dirac distribution functions, respectively, and $\alpha^2_{k\sigma}F(\omega)$ is the Eliashberg function.[3] In the present analyses, $\alpha^2_{k\sigma}$ is treated as a constant and is optimized to reproduce the observed self-energy. A calculated phonon density of states of Ni (Ref. 24) is used for $F(\omega)$.

The decreases of the Im $\Sigma^\downarrow$ for E > −40 meV for the $\Sigma_{2\downarrow}$ and $\Sigma_{1\downarrow}$ bands are well explained by the energy dependence of $\Gamma^\downarrow_{el\text{-}ph}$ [the solid curves in Fig. 4(a)]. Figure 4(b) exhibits the theoretical Re $\Sigma^\downarrow$, which is calculated to satisfy the Kramers-Kronig relation with Im $\Sigma^\downarrow$. Note that the experimental Re $\Sigma^\downarrow$s are well reproduced by the theoretical ones. These results demonstrate that the electron-phonon interaction produces the kink structure.

The electron-phonon coupling constant (λ) can be evaluated by $\lambda = |\partial\ \mathrm{Re}\ \Sigma^\sigma/\partial\omega|_{\omega=0}$. These values are summarized in Table I, together with mass enhancement factors due to electron correlation (η), and evaluated effective mass (m^*), which are discussed later. We have calculated λ using the experimental Re $\Sigma^\downarrow$ [dashed lines in Fig. 4(b)],[28] and have obtained $\lambda = 0.57 \pm 0.06$ and 0.33 ± 0.05 for the $\Sigma_{2\downarrow}$ and $\Sigma_{1\downarrow}$ bands, respectively. However, the electron-phonon interaction is much weaker in the $\Sigma_{1\uparrow}$ band ($\lambda \sim 0$).

We first discuss the magnitude of λ in relation to the d weight, since d electrons are on average located close to the

TABLE I. The electron-phonon coupling constant (λ), mass enhancement factor due to electron correlation (η), and effective mass (m^*) compared with the mass given by the band-structure calculation (m_b).

Bands	λ	η	$m^*/m_b=(1+\lambda)\eta$
$\Sigma_{2\downarrow}$	0.57±0.06	1.8±0.2	2.8±0.2
$\Sigma_{1\uparrow}$	~0	2.2±0.1	2.2±0.1
$\Sigma_{1\downarrow}$	0.33±0.05	1.4±0.1	1.9±0.1

Ni ions compared with *sp* electrons, and are easily influenced by the motion of the ions.[29] On the basis of a LSDA calculation,[30] the $\Sigma_{2\downarrow}$ band is purely *d* like, while the *d* weight at E_F for the $\Sigma_{1\downarrow}$ band, ~90%, is smaller due to *s*-*d* hybridization. Although the $\Sigma_{1\uparrow}$ and $\Sigma_{1\downarrow}$ bands have the same symmetry, the *d* weight in the $\Sigma_{1\uparrow}$ band at E_F was slightly smaller, at ~80%, than that in the $\Sigma_{1\downarrow}$ band, due to exchange splitting. Although the reduced *d* weight in the majority-spin Σ_1 band seems to explain the result qualitatively, the difference, ~10%, is rather too small to account for the significant differences between the kink structures in the Σ_1 bands. Since Ni ARPES spectra deviate from the LSDA results due to spin-dependent electron correlation,[18–20,31] we should incorporate this effect in our explanation.

Next, in order to obtain insight into the interplay between the electron-phonon interaction and electron correlation, we have evaluated the effective mass enhancement of quasiparticles due to electron correlation for the Σ_1 and Σ_2 bands. The observed Fermi velocities (v_F^{ARPES}), which have been evaluated using the solid lines in Figs. 2(c) and 3(b), are small compared with the corresponding LSDA values (v_F^{LSDA}) by a factor of $v_F^{\mathrm{ARPES}}/v_F^{\mathrm{LSDA}}\sim 47-69\%$, consistent with the observed narrowing of the experimental Ni 3*d* band width.[5–9] We have estimated the ratio of the Fermi vectors obtained from the ARPES experiment (k_F^{ARPES}) and the LSDA calculation (k_F^{LSDA}) as $k_F^{\mathrm{ARPES}}/k_F^{\mathrm{LSDA}}=1.0\pm0.1$ and 0.9 ± 0.1 for the Σ_1 and Σ_2 bands, respectively, which is in good agreement with the previous ARPES study.[22] Now the mass enhancement factors due to electron correlation (η) can be evaluated using $\eta=(k_F^{\mathrm{ARPES}}/k_F^{\mathrm{LSDA}})(v_F^{\mathrm{LSDA}}/v_F^{\mathrm{ARPES}})$. The η value for the $\Sigma_{1\downarrow}$ band is only 60% of that for the $\Sigma_{1\uparrow}$ band, and the η value for the *d*-like $\Sigma_{2\downarrow}$ band is larger than that for the *s*-*d* hybridized $\Sigma_{1\downarrow}$ band. These results exhibit a significant spin and energy-band dependence of electron correlation.

Now we move to a discussion of the effective mass enhancement $m^*/m_b=(1+\lambda)\eta$ due to both the electron-phonon interaction and electron correlation, where m_b represents the electron mass given by the LSDA calculation. The present results for m^*/m_b (1.9–2.8) agree well with those (1.8–2.3) from a de Haas–van Alphen measurement.[32] It should be noted, however, that we have provided the first estimates of the details of the origin of the effective mass enhancement for each of the energy bands. If one compares $\Sigma_{2\downarrow}$ and $\Sigma_{1\downarrow}$, both the electron-phonon interaction and the electron correlation become stronger in the $\Sigma_{2\downarrow}$ band. On the other hand, if one compares the $\Sigma_{1\uparrow}$ and $\Sigma_{1\downarrow}$ bands, a significant difference is recognized. The effective mass enhancement is mainly derived from electron correlation ($\eta\sim2.2, 1+\lambda\sim1$) in the $\Sigma_{1\uparrow}$ band, while both the electron-phonon interaction ($1+\lambda\sim1.3$) and electron correlation ($\eta\sim1.4$) contribute in the $\Sigma_{1\downarrow}$ bands. These interactions contribute to the effective mass of a quasiparticle depending on the energy band and spin direction. We should therefore take into account the interplay of these many-body interactions to explain fine photoelectron spectral features near E_F.[33]

We can also examine the electron-electron interaction via the lifetime broadening. From the fit of the observed $|2\,\mathrm{Im}\,\Sigma^\sigma|$ with $\Gamma^\sigma_{el\text{-}el}\cong 2\beta^\sigma[(\pi k_B T)^2+\omega^2]$ [dashed lines in Fig. 4(a)],[3] we obtained $2\beta^\uparrow\sim(1.4\pm0.3)\ \mathrm{eV}^{-1}$ and $2\beta^\downarrow\sim(0.6\pm0.2)\ \mathrm{eV}^{-1}$ for the $\Sigma_{1\uparrow}$ and $\Sigma_{1\downarrow}$ bands, respectively, which confirms that quasiparticles with up-spin are strongly scattered compared to those with down spin.[18–20]

Recently, Schäfer *et al.* have reported a kink structure at −160 meV derived from the electron-magnon interaction in a surface state of Fe(110) grown on W(110).[34] In the case of Ni, the kink structure due to electron-magnon interaction is expected to be −130 meV,[35] which has not been observed in the present study. Further exploration over a wider region of *k* space would be desirable.

In summary, we have performed a high-resolution ARPES study of Ni(110). A kink structure at −40 meV is observed in the $\Sigma_{2\downarrow}$ and $\Sigma_{1\downarrow}$ bands, but is absent in the $\Sigma_{1\uparrow}$ band. Based on quantitative analyses of the self-energies, we have determined that the kink structure is derived from the electron-phonon interaction. We have also evaluated the effective electron mass enhancement due to the electron-phonon interaction and electron correlation. Each of these interactions contributes to the effective mass of the quasiparticles depending on the energy band and spin direction. These results indicate the importance of the interplay of these many-body interactions in the interpretation of fine spectral features near E_F.

This work was partly supported by a Grant-in-Aid for COE Research (No. 13CE2002) by the Ministry of Education, Science, and Culture of Japan. We acknowledge Professor T. Oguchi (Hiroshima University), and Dr. Y. Aiura (AIST) for valuable discussion on the band-structure calculation, and the ARPES of Ni, respectively. We thank the Materials Science Center, N-BARD, Hiroshima University for supplying liquid helium. The synchrotron radiation experiments have been done under the approval of HSRC (Proposal No. 03-A-42).

*Corresponding author: kshimada@hiroshima-u.ac.jp

[1] S. Hüfner, *Photoelectron Spectroscopy*, 3rd ed. (Springer-Verlag, Berlin, 2003).
[2] A. Damascelli, Z. Hussain, and Z. X. Shen, Rev. Mod. Phys. **75**, 473 (2003), and references therein.
[3] T. Valla, A. V. Federov, P. D. Johnson, and S. L. Hulbert, Phys. Rev. Lett. **83**, 2085 (1999).
[4] J. Shi, S.-J. Tang, B. Wu, P. T. Sprunger, W. L. Yang, V. Brouet, X. J. Zhou, Z. Hussain, Z.-X. Shen, Z. Zhang, and E. W. Plummer, Phys. Rev. Lett. **92**, 186401 (2004), and references therein.
[5] E. Dietz, U. Gerhardt, and C. J. Maetz, Phys. Rev. Lett. **40**, 892 (1978).
[6] D. E. Eastman, F. J. Himpsel, and J. A. Knapp, Phys. Rev. Lett. **40**, 1514 (1978).
[7] F. J. Himpsel, J. A. Knapp, and D. E. Eastman, Phys. Rev. B **19**, 2919 (1979).
[8] W. Eberhardt and E. W. Plummer, Phys. Rev. B **21**, 3245 (1980).
[9] K. Ono, A. Kakizaki, K. Tanaka, K. Shimada, Y. Saitoh, and T. Sendohda, Solid State Commun. **107**, 153 (1998).
[10] C. S. Wang and J. Callaway, Phys. Rev. B **15**, 298 (1977).
[11] F. Weling and J. Callaway, Phys. Rev. B **26**, 710 (1982).
[12] S. Hüfner and G. K. Wertheim, Phys. Lett. **A51**, 299 (1975).
[13] R. Clauberg, W. Gudat, E. Kisker, E. Kuhlmann, and G. M. Rothberg, Phys. Rev. Lett. **47**, 1314 (1981).
[14] Y. Sakisaka, T. Komeda, M. Onchi, H. Kato, S. Masuda, and K. Yagi, Phys. Rev. Lett. **58**, 733 (1987).
[15] A. Kakizaki, J. Fujii, K. Shimada, A. Kamata, K. Ono, K. H. Park, T. Kinoshita, T. Ishii, and H. Fukutani, Phys. Rev. Lett. **72**, 2781 (1994).
[16] J. Kanamori, Prog. Theor. Phys. **30**, 275 (1963).
[17] D. R. Penn, Phys. Rev. Lett. **42**, 921 (1979).
[18] A. Liebsch, Phys. Rev. Lett. **43**, 1431 (1979); A. Liebsch, Phys. Rev. B **23**, 5203 (1981).
[19] L. Kleinman, Phys. Rev. B **19**, 1295 (1979); L. Kleinman and K. Mednick, Phys. Rev. B **24**, 6880 (1982).
[20] G. Treglia, F. Ducastelle, and D. Spanjaard, Phys. Rev. B **21**, 3729 (1980); G. Tréglia, F. Ducastelle, and D. Spanjaard, J. Phys. (Paris) **43**, 341 (1982).
[21] K. Shimada, M. Arita, Y. Takeda, H. Fujino, K. Kobayashi, T. Narimura, H. Namatame, and M. Taniguchi, Surf. Rev. Lett. **9**, 529 (2002).
[22] P. Aebi, T. J. Kreutz, J. Osterwalder, R. Fasel, P. Schwaller, and L. Schlapbach, Phys. Rev. Lett. **76**, 1150 (1996).
[23] F. J. Himpsel, K. N. Altmann, G. J. Mankey, J. E. Ortega, and D. Y. Petrovykh, J. Magn. Magn. Mater. **200**, 456 (1999), and references therein.
[24] R. J. Birgeneau, J. Cordes, G. Dolling, and A. D. B. Woods, Phys. Rev. **136**, A1359 (1964).
[25] N. V. Smith, P. Thiry, and Y. Petroff, Phys. Rev. B **47**, 15476 (1993).
[26] T.-C. Chiang, Chem. Phys. **251**, 133 (2000).
[27] S. Sahrakorpi, M. Lindroos, and A. Bansil, Phys. Rev. B **66**, 235107 (2002).
[28] The gradients of the observed $\mathrm{Re}\,\Sigma^{\downarrow}$ are estimated for $E > -15$ meV. The analysis is equivalent to evaluate ratios of the gradient of the dashed line, $(dE/dk)_d$, and solid line, $(dE/dk)_s$, in Fig. 2(c) and Fig. 3(b); $1+\lambda=(dE/dk)_s(dE/dk)_d$.
[29] G. D. Gaspari and B. L. Gyorffy, Phys. Rev. Lett. **28**, 801 (1972).
[30] T. Oguchi (private communication).
[31] F. Manghi, V. Bellini, J. Osterwalder, T. J. Kreutz, P. Aebi, and C. Arcangali, Phys. Rev. B **59**, R10409 (1999).
[32] E. I. Zornberg, Phys. Rev. B **1**, 244 (1970).
[33] In our ARPES experiments on Cu(110) (unpublished), the kink structure and effective mass enhancement of the Σ_1 band, mainly derived from the *sp* states, are explained very well by the electron-phonon interaction. Electron correlation is not significant in the Cu case.
[34] J. Schäfer, D. Schrupp, E. Rotenberg, K. Rossnagel, H. Koh, P. Blaha, and R. Claessen, Phys. Rev. Lett. **92**, 097205 (2004).
[35] H. A. Mook and D. McK. Paul, Phys. Rev. Lett. **54**, 227 (1985).